GEOPHYSICS, VOL. 57, NO. 6 (JUNE 1992); P. 815–822, 9 FIGS.

Residual shot profile migration

Wook B. Lee* and Lin Zhang‡

ABSTRACT

We have developed a residual shot profile migration technique, which consists of dip-corrected residual normal moveout (NMO) and depth restretching. The dip-corrected residual NMO equation and the depth restretching equation were derived by generalizing Al-Yahya's residual NMO equation. Using the dip-correction residual NMO equation, velocity errors can be estimated more accurately than without the dip correction term in the residual NMO equation. Residual shot profile migration was applied to migrated prestack data in a manner similar to conventional processing by cascading residual velocity analysis, residual NMO, and stack and depth stretching. With residual migration, we can either avoid remigration of the original prestack data or reduce the number of iterations required to produce a satisfactory image. Residual migration is efficient enough to be implemented on a workstation. Significant improvement in imaging to cases (a pinchout and salt top and bottom) is demonstrated using synthetic and field data examples.

INTRODUCTION

It is well known that velocity errors have a great impact on prestack migration. However, it is difficult to quantify migration velocity errors to update the velocity model. This is often given as one of the prime reasons for the failure of prestack depth migration to produce superior results over conventional processing. The velocity errors result in residual normal moveout (NMO) and residual zero-offset migration errors. In this paper, we discuss residual processing to correct both of these effects.

As part of prestack depth migration, residual velocity analysis can be employed to quantify velocity errors and update velocity models. Two approaches in residual velocity analysis have been discussed in the literature: depth-focusing and residual moveout. Yilmaz and Chambers (1984) introduced depth-focusing, and many others (Faye and Jeannot, 1986; Cox et al., 1988; MacKay and Abma, 1989) have expanded the idea. It has been shown that depth-focusing can provide a focused seismic section. However, there are drawbacks: (1) It requires several iterations of prestack migration. (2) It is based on S-G (finite difference) migration, which is relatively slow and dip-limited. (3) Depth focusing based only on stacking power can be an ambiguous measure of velocity error. The most important issue is that the remigration of prestack data is very expensive. So in many cases, residual migration may be a better alternative unless average velocity errors are greater than 10 percent.

Al-Yahya (1989) discussed residual velocity analysis by iterative profile migration. He measured the velocity errors by estimating the curvature of residual moveout. His velocity scanning was based on the residual NMO equation for horizontal reflectors. Common offset migration followed by a residual NMO search in the common midpoint (CMP) domain has been suggested as a residual velocity analysis tool for migrated prestack data (Sattlegger et al., 1980; Deregowski, 1990). All these approaches ignore the dip effect on the residual moveout. We have derived generalized equations for dip-corrected residual NMO and depth restretching for dipping reflectors.

In a multifold seismic experiment, a small portion of the subsurface is illuminated by a collection of shot-receiver pairs, as shown in Figure 1. Imaging of such reflection data can be accomplished by the prestack depth migration of individual shot records followed by stacking the migrated traces at common-reflection points (CRP). When migrated correctly, the image of the subsurface under a surface location should show the consistent structure. The alignment of images in a CRP gather takes place regardless of structure and shot locations. When migrated incorrectly, the images of the subsurface will show either a hyperbolic or an elliptical residual moveout due to migration velocity errors.

Figure 2 shows three CRP gathers of a field data set. Moveout trajectories are curved upward or downward if the migration velocities are lower or higher than actual veloci-

Manuscript received by the Editor February 19, 1991; revised manuscript received October 23, 1991.
*Unocal Science and Technology Division, 5460 E. La Palma Ave., Anaheim, CA 92807.
‡Department of Geophysics, Stanford University, Stanford, CA 94305-2215.

ties. Residual shot profile migration using residual NMO equations can correct under- or over-migration of migrated shot profiles.

In the following sections, we will first introduce the dip-corrected residual NMO equation and the depth restretch equation and discuss the influence of structural dips on measuring velocity errors. Then we will show synthetic and field data examples of moveout corrections and depth restretching to demonstrate the performance of the residual processing algorithms.

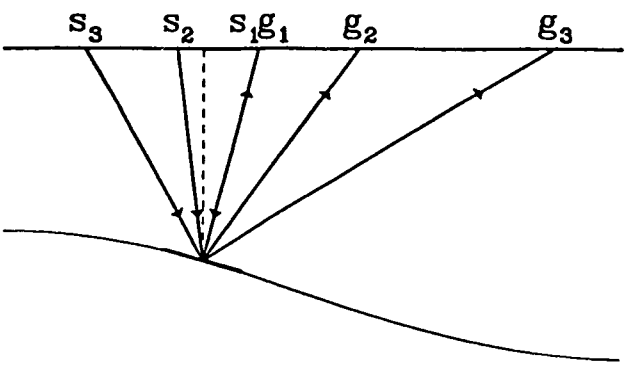

FIG. 1. Common-Reflection Point Geometry—A portion of subsurface is illuminated by shots at different offsets in a seismic experiment.

DIP-CORRECTED RESIDUAL NMO EQUATION AND DEPTH RESTRETCH EQUATION

The dip-corrected residual NMO equation and depth restretch equation relate the actual reflector depth z to the apparent reflector depth z_m and apparent offset a, where a is the distance between the shot and the surface location of a reflection point (a will be referred to as "offset" in this paper). Al-Yahya (1989) derived the following residual NMO equation for horizontal reflectors.

$$z_m^2 = \gamma^2 z^2 + (\gamma^2 - 1)a^2, \tag{1}$$

where

$$\gamma = \frac{s}{s_m},$$

The term s is the actual average medium slowness, and s_m is the average slowness used in migration.

Equation (1) contains only the second-order terms in offset as is the case in the NMO equation. Consequently, moveout trajectories are symmetric at the CMP location.

For dipping reflectors, as shown in Figure 3, the residual NMO equation contains one more parameter, b, the distance between the receiver and the surface location of the reflector. The following equation was derived by Al-Yahya (1989).

$$z_m^2 = \gamma^2 \frac{X}{4} - \frac{(a^2 + b^2)}{2} + \frac{(a^2 - b^2)^2}{4X\gamma^2}, \tag{2}$$

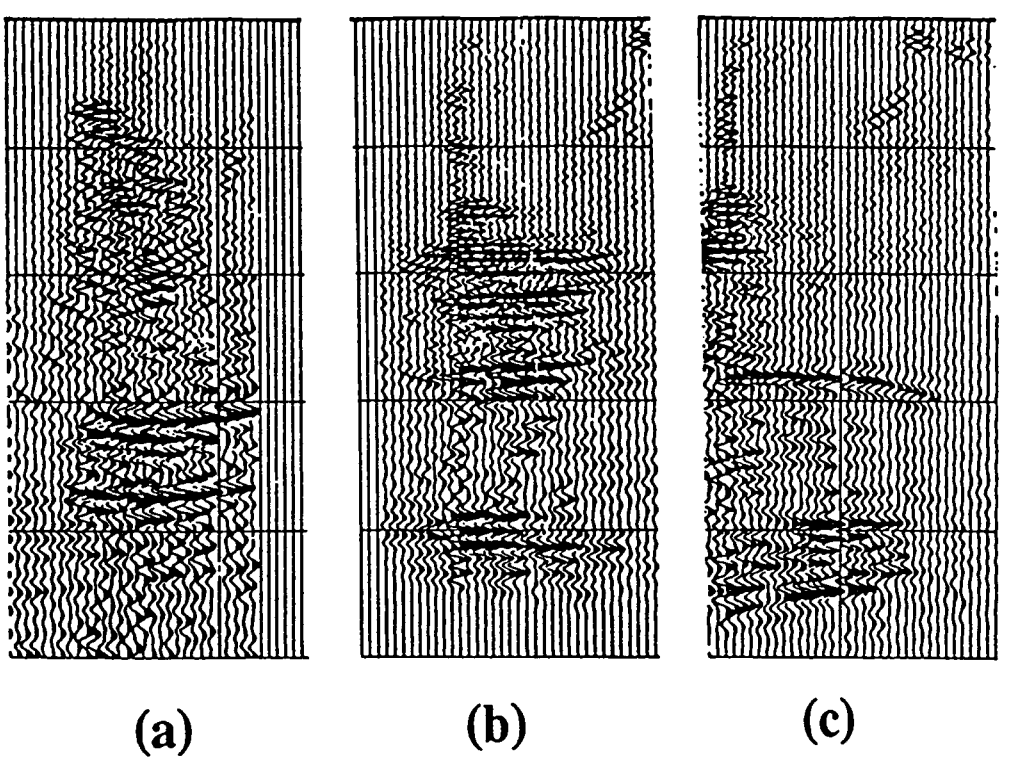

FIG. 2. Common-Reflection Point gathers—field data example, migration velocity is (a) lower than, (b) approximately equal to, (c) higher than the actual velocity.

where

$$X = 2z^2 + a^2 + b^2 + 2\sqrt{z^4 + (a^2 + b^2)z^2 + b^2a^2}.$$

As a result of shot profile migration, the signals recorded at different receivers are averaged together. The parameter b becomes an unknown. For horizontal reflectors, b is always equal to a. For dipping reflectors, however, this is not the case. Under the assumption of straight rays, b is a function of offset a, dipping angle θ, and the reflector depth z as

$$b = \frac{z(z \tan 2\theta - a)}{z + a \tan 2\theta}. \quad (3)$$

Derivation of this relationship is given in Appendix A. Obviously, the right-hand side of equation (2) is no longer a polynomial function of offset a, and moveout trajectories are no longer symmetric at the CMP location. Moveout trajectories are computed from equations (2) and (3) with θ, the dip of the reflector as a variable and a set of curves is shown in Figure 4. Notice that the apex of the trajectories moves away from the CMP location as the dipping angle of the reflector increases. The apex of the trajectories moves either to the left or to the right, depending on the sign of the dipping angle. In Appendix B, we show that the coordinates of the apex (a_0, z_0) are related to the actual depth of the reflector z satisfying the following relationship,

$$z_0^2 = \gamma^2 z^2 + (\gamma^2 - 1)a_0^2. \quad (4)$$

Assuming small dip and small offset compared to depth, equation (2) can be approximated as (see Appendix B)

$$z_m^2 = z_0^2 + (\gamma^2 - 1)\,(a - a_0)^2, \quad (5)$$

where z_0 is defined in equation (4).

Equations (4) and (5) define the moveout trajectories in a CRP gather. Equation (5) defines moveout corrections while equation (4) defines depth corrections. It is important to know that the origin of hyperbolic moveout has been moved by a_0 in equation (5). The move of the origin is due to dip. In the case of a flat reflector, equations (1) and (5) become identical.

The moveout residuals from two approximations are compared in Figure 5. Dip-corrected moveout residuals are much smaller than residuals from equation (1) for the case where 10 percent velocity errors and 30 degrees of structural dip exist.

Estimation of γ and θ

The conventional way to estimate parameters in a moveout equation is to scan over an unknown parameter, such as stacking velocity. In our case, however, the moveout equation (5) contains two unknown parameters: γ (velocity error) and θ (dip). We can scan dip and velocity error sequentially. Dip can be determined either from the migrated stack section or from the position of apex locations in the CRP gather. Velocity error can be determined by fitting curvatures to the moveout. Alternatively, we can employ the overlay method. Claerbout (1987) introduced the overlay method to perform stacking velocity analysis. In his method, a curve defined by

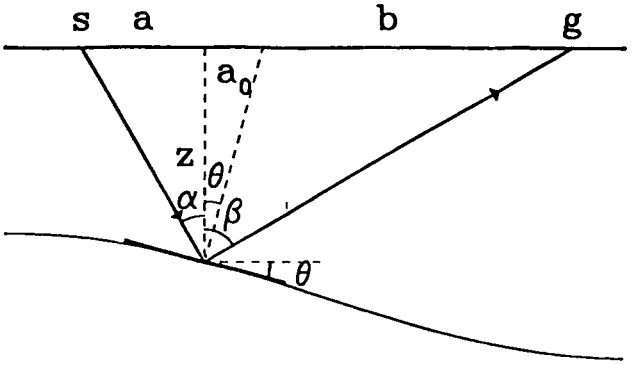

FIG. 3. Common-Reflection Point Geometry for nonhorizontal reflectors. Common reflection point (CRP) is separated from the common midpoint (CMP) by distance a_0.

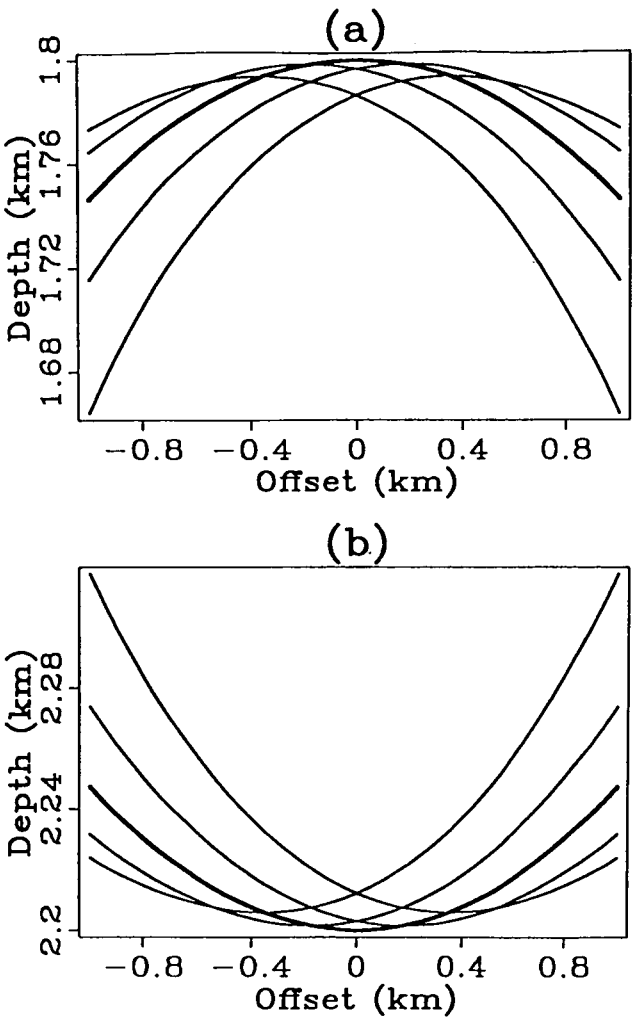

FIG. 4. Residual moveout trajectories computed using equations (2) and (3). The fat lines indicate the moveout curve for a flat reflector. With varying dip angles from −10 to +10 degrees, the moveout curve moves to the left or to the right. Migration velocity was (a) 10 percent higher and (b) 10 percent lower than the actual velocity.

the NMO equation is overlaid directly on moveout trajectories in a CMP gather. Stacking velocities are picked interactively by fitting moveout trajectories. This idea can be easily applied to our problem of two parameter fitting on a workstation. Both the scanning method and the overlay method were employed in our processing for examples.

RESULTS: A SYNTHETIC EXAMPLE

A synthetic data set was generated using the geologic model shown in Figure 6, which has flat reflectors, a dipping pinchout, and anticlines. The synthetic data set was prestack migrated with velocity models, in which migration velocities were 10 percent higher, equal to, and 10 percent lower than the correct velocities. Prestack migrated traces at a common surface location show moveout patterns that are either hyperbolic, flat, or elliptic, depending on whether the migration velocites were higher, equal to, or lower than the true velocities as shown in Figure 7. Figure 8 shows stacks of prestack migrated traces in the cases where migration velocity was exact (exact stack) and the case where it was 10 percent too slow (slow stack). Residual moveout corrections were applied to the slow stack (RMO stack), and depth restretching was applied to the RMO stack (final stack). Residual moveout corrections eliminate either hyperbolic or elliptic moveout using equations (4) and (5). Figure 8 shows the comparison of the exact stack, slow stack, RMO stack, and final stack.

Notice that moveout corrections remove the destructive interference due to curved moveout patterns so that the signal-to-noise ratio of the events increases considerably. In addition, reflectors are positioned at the correct depth location as a result of restretching.

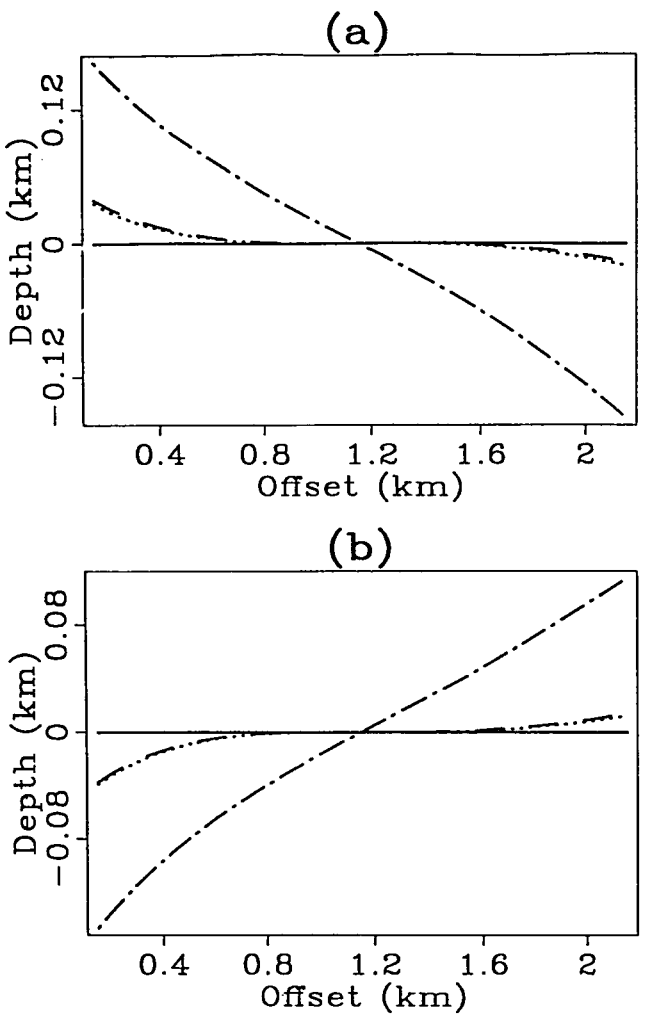

FIG. 5. Moveout residuals of various approximations are plotted as a function of offset, (a) when $\gamma = 0.9$, $z = 2$ km, and $\theta = 30$ degrees, and (b) when $\gamma = 1.1$, $z = 2$ km, and $\theta = 30$ degrees. Solid lines indicate no errors. Dot-dashed lines indicate residuals when Al Yahya's equation (1) is used. Dotted lines indicate residuals when our equations (4) and (5) are used. Dashed lines indicate residuals when more precise equation (B-6) is used.

RESULTS: A FIELD EXAMPLE

A field example shows North Sea salt tectonics. Our processing objective is to image the top and bottom of salt. Figure 9a shows a depth section from conventional time migration and time-to-depth conversion. Reflectors below the salt are fragmented and lead to misinterpretation. Figure 9b shows the result of prestack depth migration using a reasonably accurate velocity model. It shows a better focused result than time migration. The event below the salt at common-depth-point (CDP) 350 (marked as 2) indicates the opposite dip to the corresponding event in the time-migrated section. However, it may not be possible to improve any further by iterations. Figure 9c shows the result of residual migration applied to migrated CRP gathers. A distinct improvement appears at the top of salt, at reflections below salt (marked as 2) and at reflection events (marked as 1) from the internal structure of salt. Residual migration is clearly a better alternative in this case.

DISCUSSION AND CONCLUSIONS

The dip-corrected residual NMO equation and the depth restretch equation were derived by generalizing Al-Yahya's residual NMO equation. Velocity errors can be estimated more accurately by the dip-corrected residual NMO equation. The assumptions involved in our derivation are that the imaging depth is greater than the maximum offset and that reflector dips are mild.

Using equations (4) and (5), residual shot profile migration can be performed as follows: (1) migrate profiles using the current model, (2) determine γ as a function of depth using equation (5), (3) apply residual NMO and stack, and (4) restretch to depth. Remigration was not required in these procedures.

Al-Yahya (1989) described his velocity analysis using profile migration as an iterative scheme: (1) migrate profiles using the current model, (2) determine γ as a function of depth using equation (1), (3) compute average slowness from γ, (4) compute interval slowness, and (5) update the current model and go back to the loop or exit the loop. In Al-Yahya's scenario, convergence was achieved by remigrating the data with an updated model. All approaches but MacKay and Abma's (1989) require remigration.

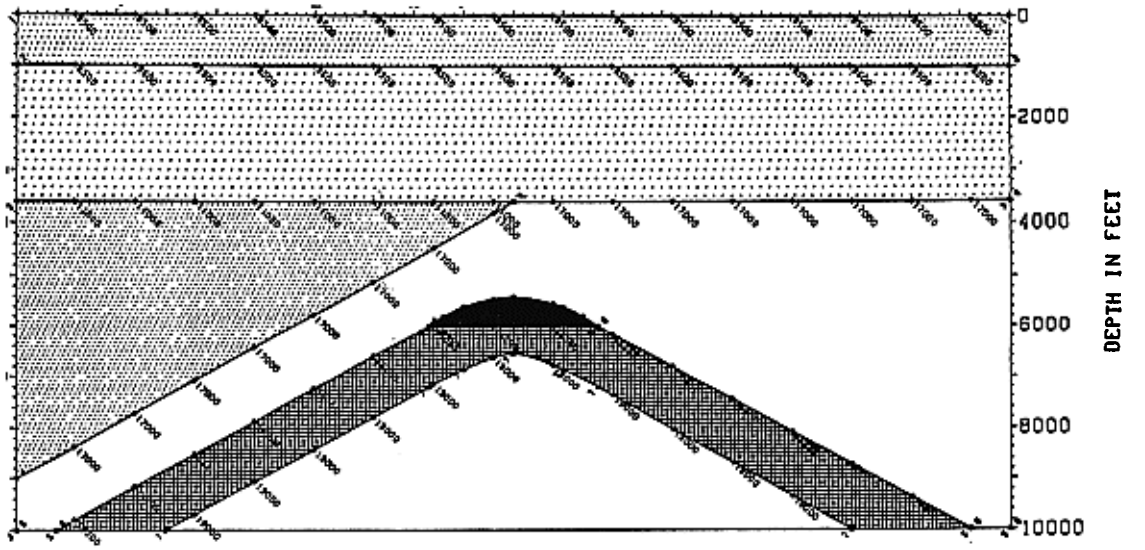

FIG. 6. The gas-cap model for the synthetic example. A trap between two anticlines contains gas, which is low velocity material.

Residual migration can be implemented on a workstation, while remigration requires a supercomputer.

More importantly, updating the velocity model may not be straightforward for geologically complex models. Further improvement in imaging may be limited by the ambiguity in updating models. Residual migration may be a better alternative for successful imaging by dip-corrected residual NMO and stacking.

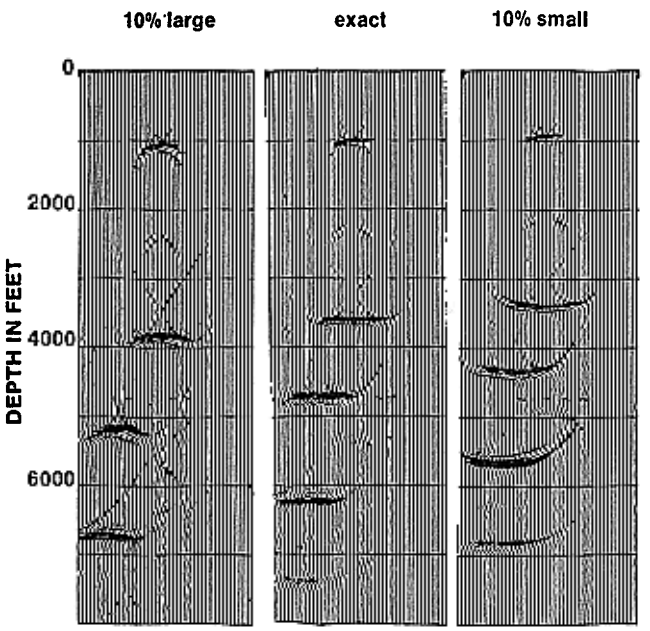

FIG. 7. CRP gathers at the corresponding surface location of the left tip of the gas trap. These CRP gathers were generated as the result of prestack migration using migration velocities (a) 10 percent higher than, (b) equal to, and (c) 10 percent lower than the actual average velocity.

We demonstrated the successful application of residual migration to a synthetic data set, which has a 10 percent velocity error with 30 degree structural dip. A field data example shows significant image enhancement of salt bottom and salt internal reflections from Platten dolomite.

ACKNOWLEDGMENTS

We wish to express our gratitude to the Unocal Science and Technology Division for permission to publish this paper. We also thank Chris von Kahrs for providing us with the synthetic data, Bob McCollom for providing his prestack depth migration result, and David DeBaun for his critical review and comments.

REFERENCES

Al-Yahya, K., 1989, Velocity analysis by iterative profile migration: Geophysics, **54**, 718–729.

Claerbout, J., 1987, Interpretation with the overlay program: Stanford Expl. Proj. Rep. 51, 269–300.

Cox, H. L. H., Oomes, F. P. J., Wapenaar, C. P. A. and Berkhout, A. J., 1988, Verification of macro subsurface models using a shot record approach: 58th Ann. Internat. Mtg., Soc. Expl. Geophys., Expanded Abstract, 904–908.

Deregowski, S. M., 1990, Common-offset migrations and velocity analysis: First Break, **8**, no. 6, 225–234.

Faye, J. P., and Jeannot, J. P., 1986, Prestack migration velocities from focusing depth analysis: 56th Ann. Internat. Mtg., Soc. Expl. Geophys., Expanded Abstract, 438–440.

MacKay, S., and Abma, R., 1989, Refining prestack depth migration images without remigration: Presented at the 61st Europ. Assn. Expl. Geophys. Mtg., Abstract, 98.

Sattlegger, J. W., Stiller, P. K., Echterhoff, J. A., and Hentschke, M. K., 1980, Common offset plane migration (COPMIG): Geophys. Prosp., **28**, 859–871.

Yilmaz, O., and Chambers, R., 1984, Migration velocity analysis by Wavefield extrapolation: Geophysics, **49**, 1664–1674.

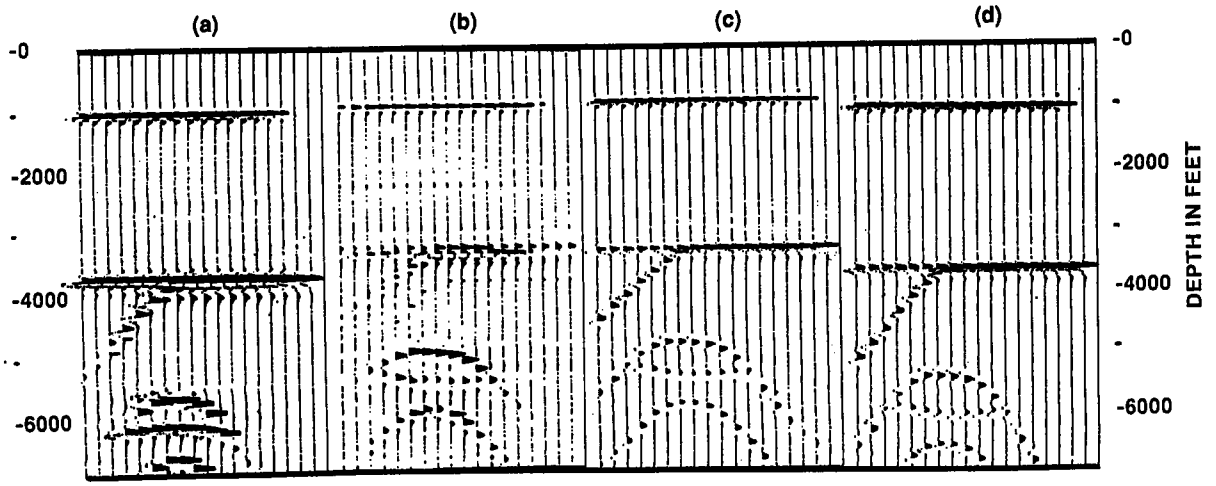

FIG. 8. Stacks of prestack migrated CRP gathers when migration velocity was (a) exact (exact stack), (b) 10 percent lower than the actual velocity (slow stack), (c) after residual moveout corrections applied to slow stack (RMO stack), and (d) after depth restretch applied to RMO stack (final stack).

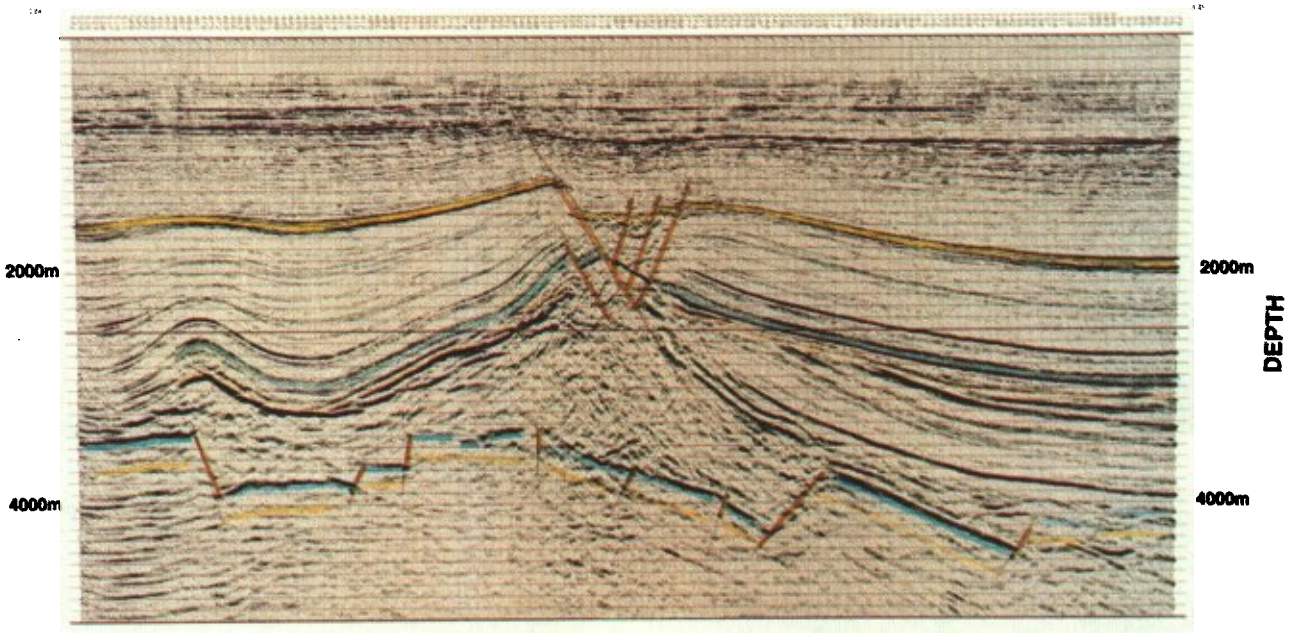

FIG. 9(a). The depth section of poststack time migration.

FIG. 9(b). The depth section of prestack depth migration.

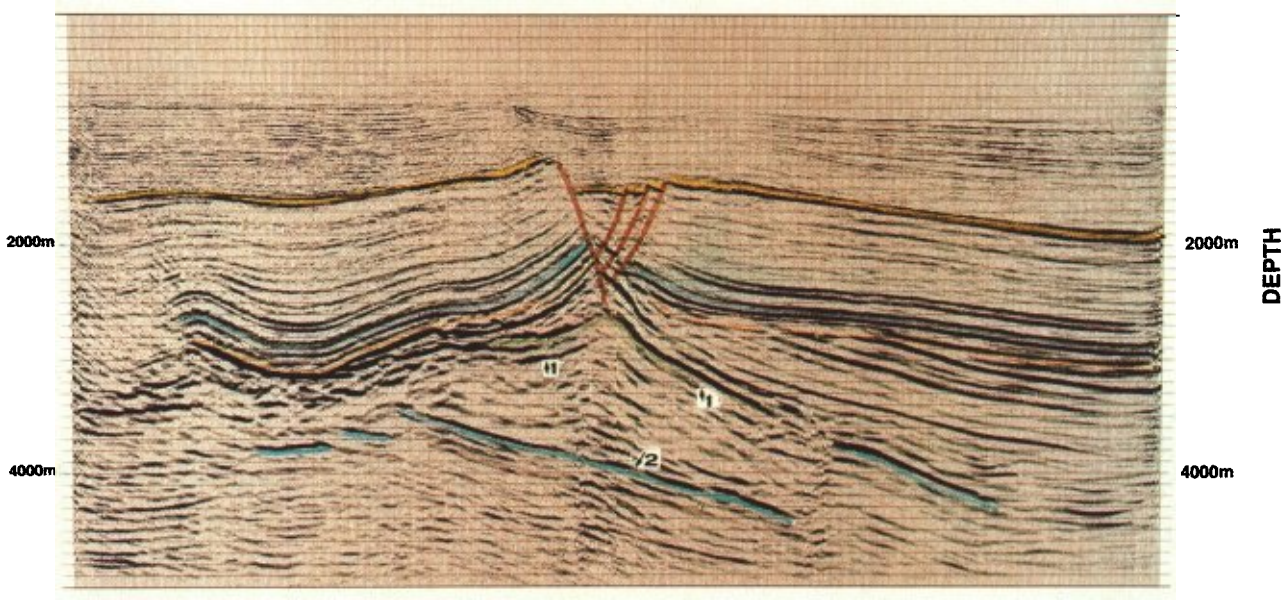

FIG. 9(c). The depth section of prestack depth migration plus residual migration.

APPENDIX A

DERIVATION OF EQUATION (3)

According to the geometry shown in Figure 3, we have the following relations:

$$\beta = 2\theta - \alpha, \tag{A-1a}$$

$$a = z \tan \alpha, \tag{A-1b}$$

$$b = z \tan \beta, \tag{A-1c}$$

$$a_0 = z \tan \theta. \tag{A-1d}$$

Solving equations (A-1), we obtain

$$b = z \tan \left[2\theta - \arctan\left(\frac{a}{z}\right)\right]$$

$$= z\left(\frac{z \tan 2\theta - a}{z + a \tan 2\theta}\right). \tag{A-2}$$

APPENDIX B

DIP-CORRECTED RESIDUAL NMO EQUATION AND DEPTH RESTRETCH EQUATION

Al-Yahya (1989) derived equation (1) from equation (2):

$$z_m^2 = \gamma^2 \frac{X}{4} - \frac{a^2 + b^2}{2} + \frac{(a^2 - b^2)^2}{4X\gamma^2},$$

where

$$X = 2z^2 + a^2 + b^2 + 2\sqrt{z^4 + (a^2 + b^2)z^2 + b^2a^2}.$$

We are going to derive dip-corrected equations (4) and (5). Rewriting the expression in equation (2) under the $\sqrt{}$ as

$$\left(z^2 + \frac{a^2 + b^2}{2}\right)^2 - \frac{1}{4}(a^2 - b^2)^2.$$

Then

$$X = 2\left(z^2 + \frac{a^2 + b^2}{2}\right)\left(1 + \sqrt{1 - \frac{1}{4}\varepsilon^2}\right), \tag{B-1}$$

where

$$\varepsilon^2 = \frac{(a^2 - b^2)^2}{\left(z^2 + \frac{a^2 + b^2}{2}\right)^2}.$$

Assumption 1.—Offsets a, b are small compared to depth z.

$$\varepsilon^2 \ll 1.$$

Substituting equation (B-1) into equation (2) and neglecting all terms of order ε^2, we get

$$z_m^2 = \gamma^2 z^2 + \frac{1}{2}(\gamma^2 - 1)(a^2 + b^2). \tag{B-2}$$

Assumption 2.—Small dip. Equation (A-2) becomes

$$b = 2a_0 - a,$$

and it gives

$$z_m^2 = z^2\gamma^2 + (\gamma^2 - 1)[a_0^2 + (a - a_0)^2]. \tag{B-3}$$

For zero offset,

$$b = a = a_0.$$

Substituting this relation into equation (B-3), we have

$$z_0^2 = \gamma^2 z^2 + (\gamma^2 - 1)a_0^2. \tag{B-4}$$

Now substituting equation (B-4), we can rewrite equation (B-3) as

$$z_m^2 = z_0^2 + (\gamma^2 - 1)(a - a_0)^2. \tag{B-5}$$

Let us find the second-order Taylor expansion of equation (2).

$$\left.\frac{\partial z_m^2}{\partial a}\right|_{a = a_0} = 0. \tag{B-6a}$$

$$\left.\frac{\partial z_m^2}{\partial a^2}\right|_{a = a_0} = 2(\gamma^2 - 1) + 2(\gamma^2 - 1)^2 \frac{a_0^2}{z_0^2 + a_0^2}. \tag{B-6b}$$

Including second-order terms in Taylor expansion of equation (B-2),

$$z_m^2 = z_0^2 + \left.\frac{\partial z_m^2}{\partial a}\right|_{a = a_0}(a - a_0) + \frac{1}{2}\left.\frac{\partial z_m^2}{\partial a^2}\right|_{a = a_0}(a - a_0)^2$$

$$= z_0^2 + (\gamma^2 - 1)(a - a_0)^2$$

$$+ 2(\gamma^2 - 1)^2 \frac{a_0^2}{z_0^2 + a_0^2} \tag{B-6c}$$